Nuclear structure effects on photoproduction in peripheral and ultraperipheral isobar collisions

Shuo Lin

Department of Modern Physics,
University of Science and Technology of China

Based on:

S. Lin,R.J. Wang, J.F. Wang, H.J. Xu, S. Pu and Q. Wang, Phys.Rev.D 107 (2023), 054004

S. Lin,J.Y.Hu,H.J. Xu, S. Pu and Q. Wang, in preparation

Spicy Gluons 2024: Workshop for Young Scientists on the quark-gluon matter in extreme conditions

Outline

- **Introduction & Motivation**
- **Nuclear structure effects on photoproduction of di-electrons in peripheral isobar collisions**
- **Nuclear deformation effects on photoproduction of ρ in ultraperipheral isobar collisions**
- **Summary**

Strong EB fields in HIC

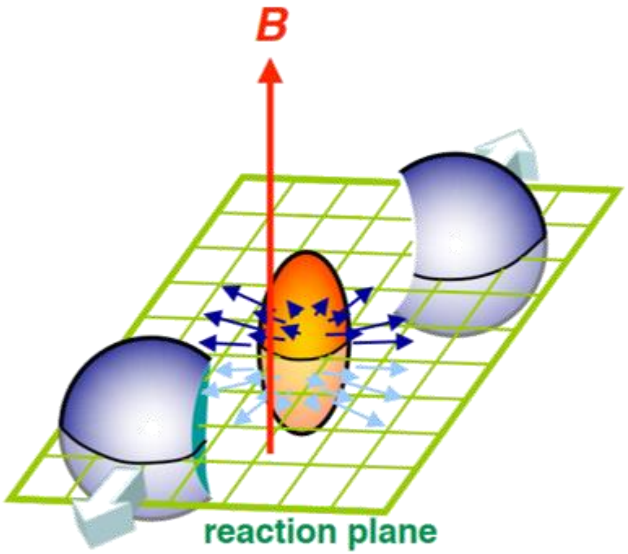

Schwinger Effect

J.S. Schwinger,Phys. Rev. 82 (1951) 664P. Copinger, K. Fukushima, and S. Pu, Phys. Rev. Lett. 121, 261602 (2018)
P. Copinger and S. Pu, Int. J. Mod. Phys. A 35, 2030015 (2020)
……

Vacuum birefringence

S. L. Adler, Annals Phys. 67, 599 (1971).
……

- $eB \sim \gamma Z \alpha v / b_T^2 \sim 10^{18}\text{Gauss}$

$\sqrt{s_{NN}} = 200\text{GeV}$ Au+Au

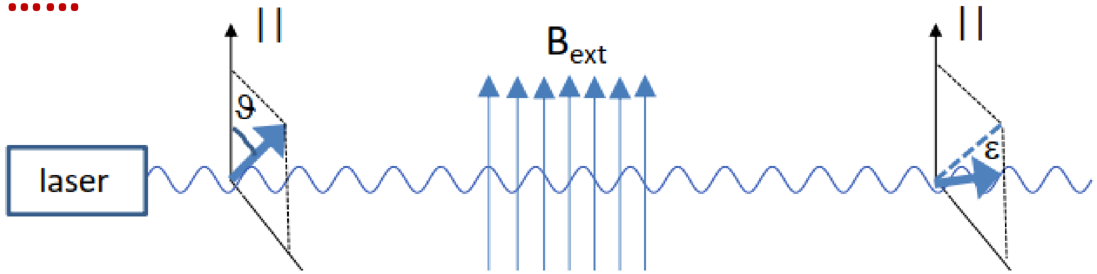

Equivalent Photon Approximation

Ultra-relativistic charged particle can produce highly Lorentz contracted electromagnetic field

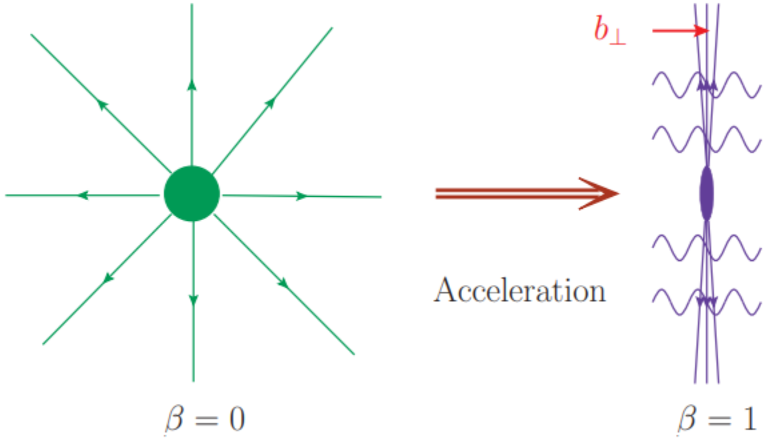

Equivalent Photon Approximation

Classical EM ⇔ Quasi-real photons

Equivalent Photon Approximation

Due to the large flux of quasi-real photon,QED effects are enhanced by the Ze

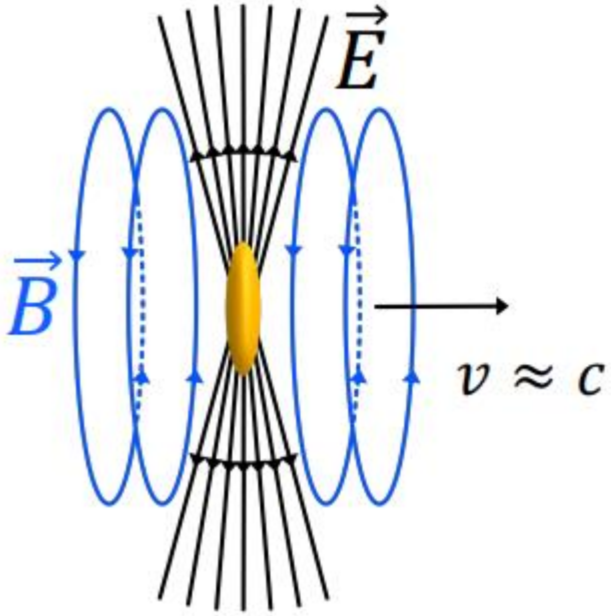

$$n(\omega) = \frac{4Z^2\alpha_e}{\omega} \int \frac{d^2k_\perp}{(2\pi)^2} k_\perp^2 \left[\frac{F(k_\perp^2 + \omega^2/\gamma^2)}{(k_\perp^2 + \omega^2/\gamma^2)} \right]^2$$

Ultraperipheral Collisions(UPC)

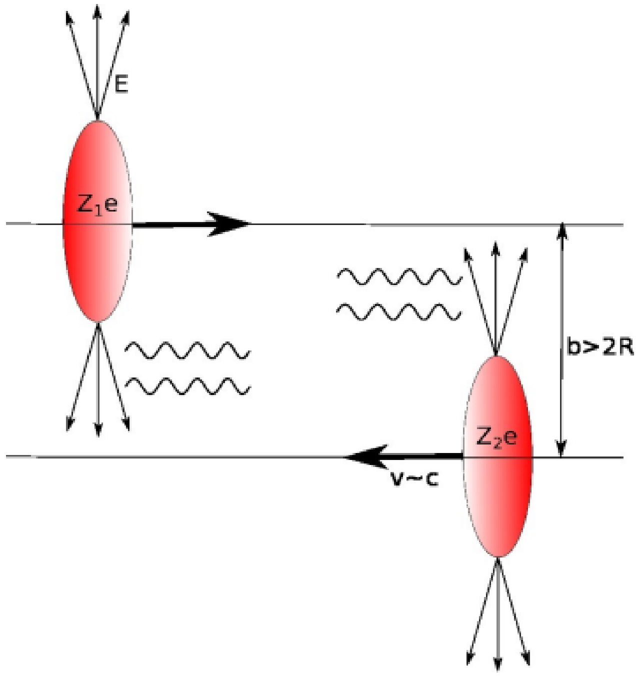

UPC: the impact parameter is larger than 2 times the radius of a nucleus

Clean background

Photoproduction in HIC

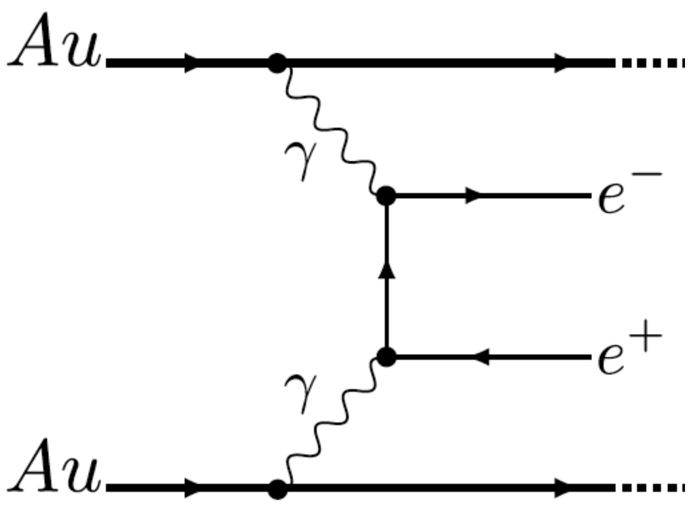

$\gamma\gamma \to l^+ l^-$

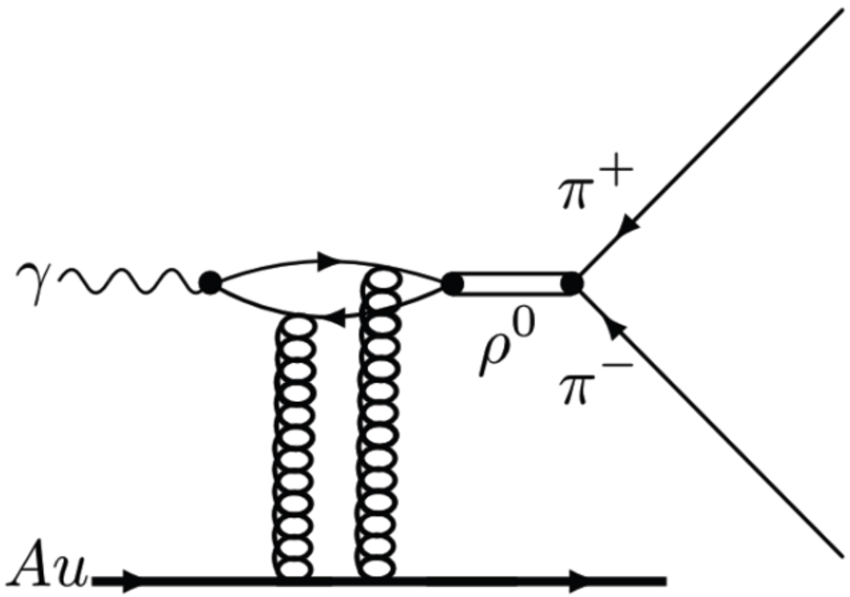

$\gamma\mathbb{P} \to \rho$

Isobar collisions

- The isobar collision was proposed to measure the chiral magnetic effect.

- Same background
- Different magnetic field

=> different CME signal

$$j_{CME} = \frac{e^2}{2\pi^2}\mu_5 \boldsymbol{B}$$

D. Kharzeev, L. McLerran, and H. Warringa, Nucl.Phys. A 803, 227 (2008)

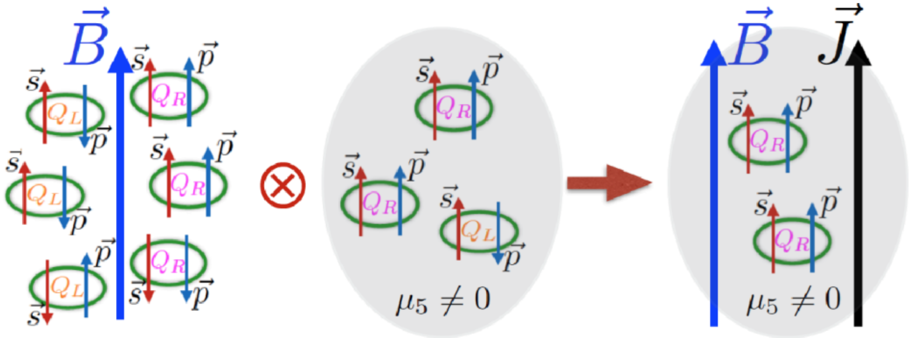

Isobar collisions

- Precision isobar data can be used to probe neutron skin thickness ,nuclear symmetry energy and nuclear deformation

Backgrounds are not identical!

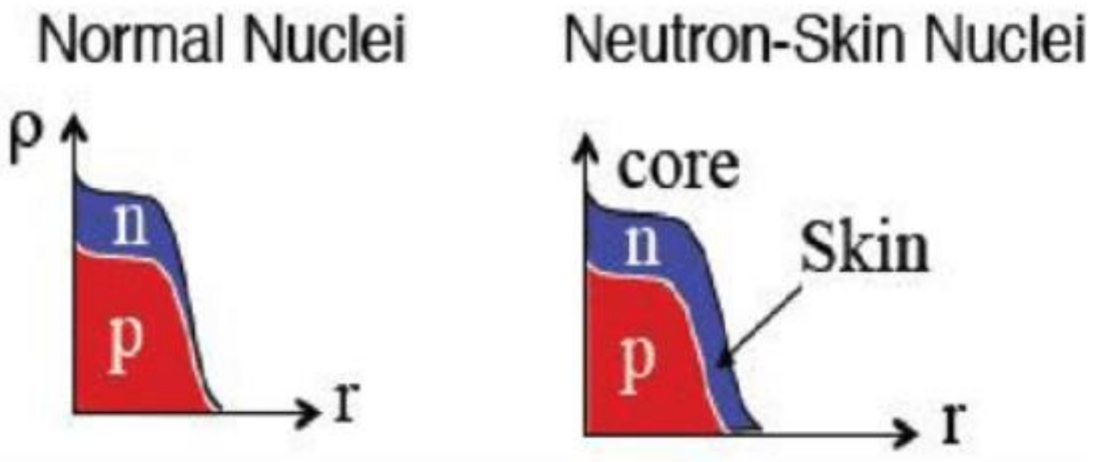

H.J. Xu, et.al., PRL121, 022301 (2018)

H. Li, H.J. Xu et.al., PRC98, 054907(2018)

C. Zhang, J. Jia, PRL128, 022301(2022)

S. Zhao, H.J. Xu, et.al, PLB839, 137838 (2023)

……

Isobar collisions

- Can nuclear structure information be reflected in the photoproduction in isobar collision ?

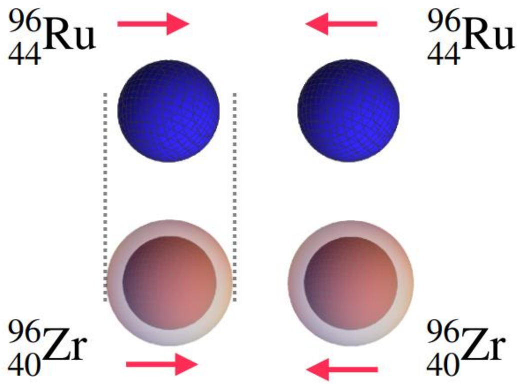

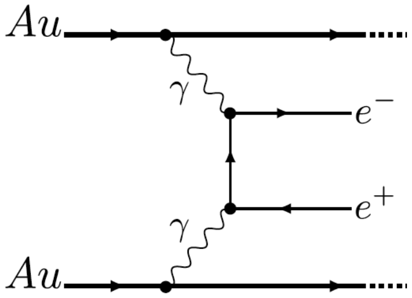

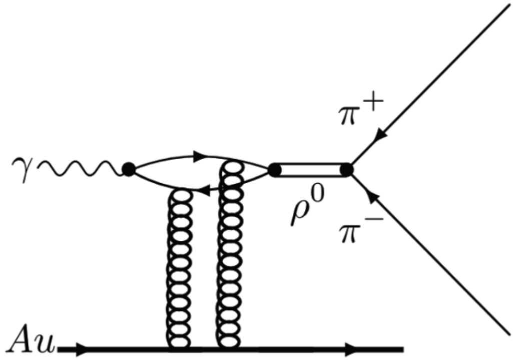

Photoproduction of di-electrons in peripheral isobar collisions

Breit-Wheeler Process

In 1934 Breit and Wheeler

DECEMBER 15, 1934 PHYSICAL REVIEW VOLUME 46

Collision of Two Light Quanta

G. BREIT* AND JOHN A. WHEELER,** *Department of Physics, New York University*

(Received October 23, 1934)

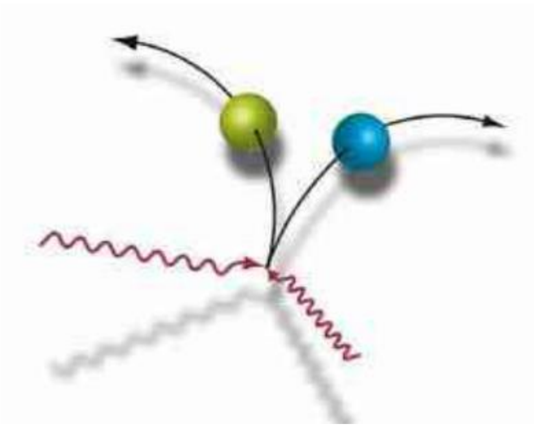

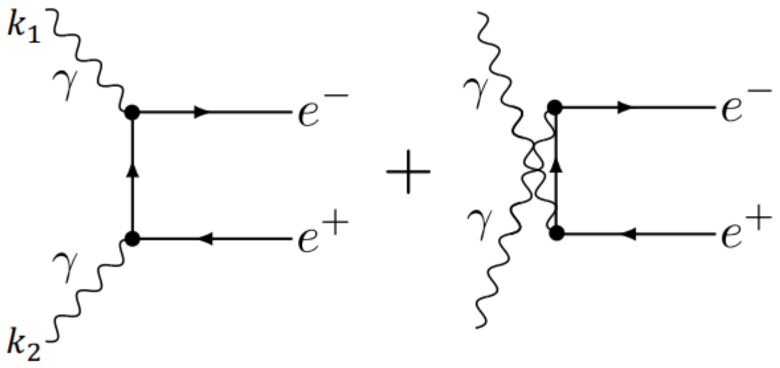

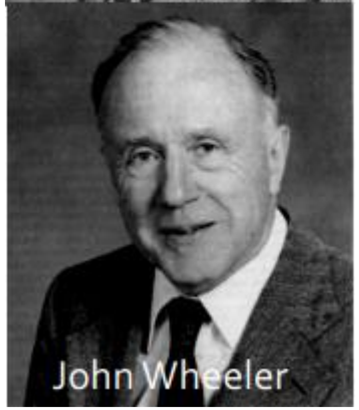

Breit-Wheeler Process

- $\gamma\gamma \rightarrow l^+l^-$ processes have been measured in UPC

STAR, J. Adam et al., Phys. Rev. Lett. 127, 052302 (2021), 1910.12400.

ATLAS, G. Aad et al., Phys. Rev. C 104, 024906 (2021), 2011.12211.

CMS, A. M. Sirunyan et al., Phys. Rev. Lett. 127, 122001 (2021), 2011.05239.

ALICE, Abbas, E et al., Eur.Phys.J.C 73 (2013)11, 2617, 1305.1467.

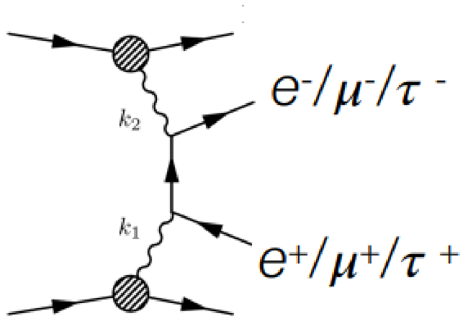

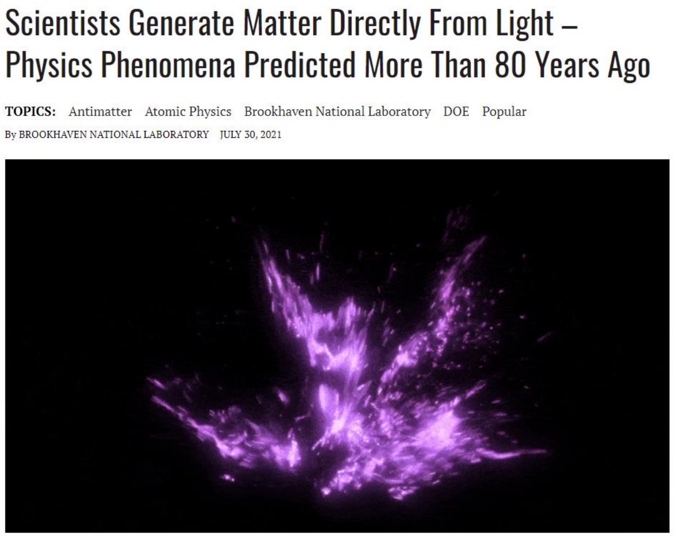

Breit-Wheeler Process

- $\gamma\gamma \to l^+l^-$ processes have also been measured in peripheral collisions ($b < 2R_A$ PC)

STAR, J. Adam et al., Phys. Rev. Lett. 121, 132301 (2018), 1806.02295.

ATLAS, M. Aaboud et al., Phys. Rev. Lett. 121, 212301 (2018), 1806.08708.

ALICE, Sebastian Lehner et al., PoS LHCP2019 (2019) 164, 1909.02508.

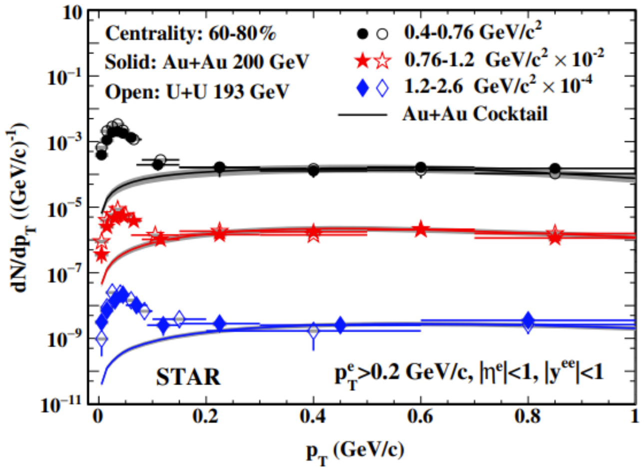

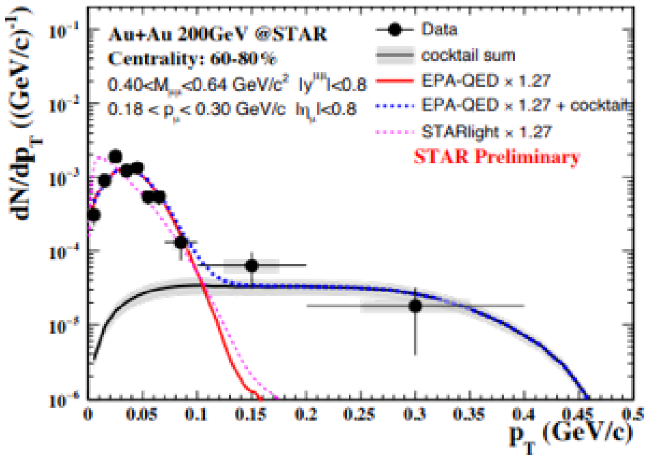

Excess above hadronic production has been observed at low transverse momentum of dileptons (P_T^{ee})

Peripheral Collisions

R.J. Wang, S. Lin, S.Pu,Y.F. Zhang, Q. Wang， Phys.Rev.D 106 (2022) 3, 034025

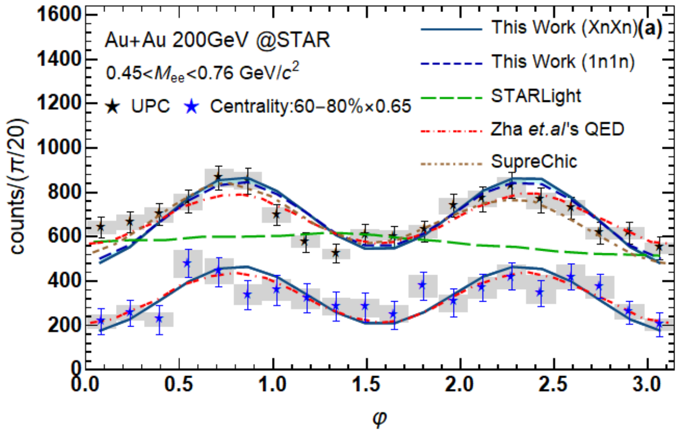

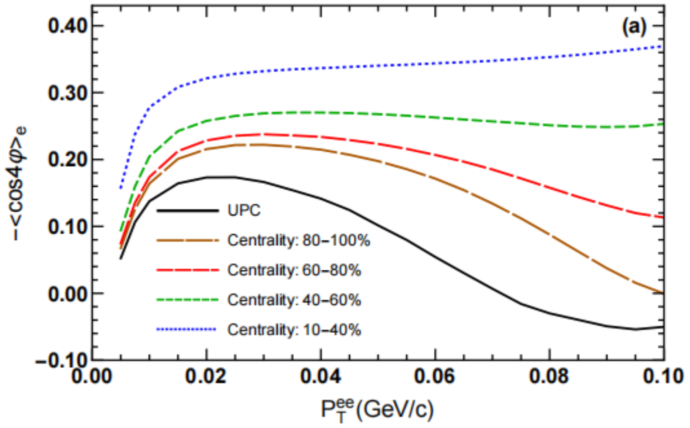

- The linear polarization information of photons is important for understanding the azimuthal asymmetry of the lepton pair.

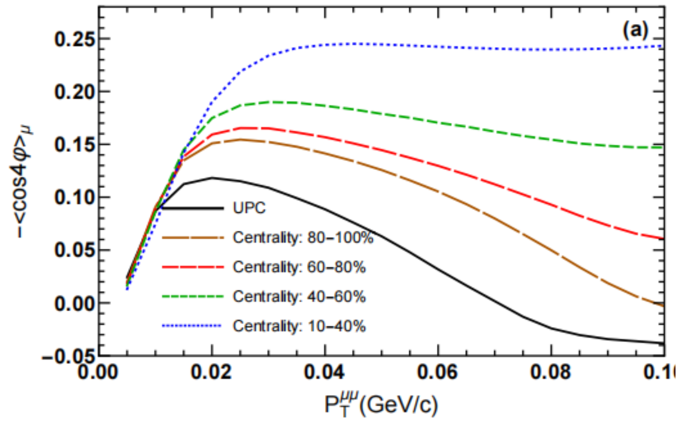

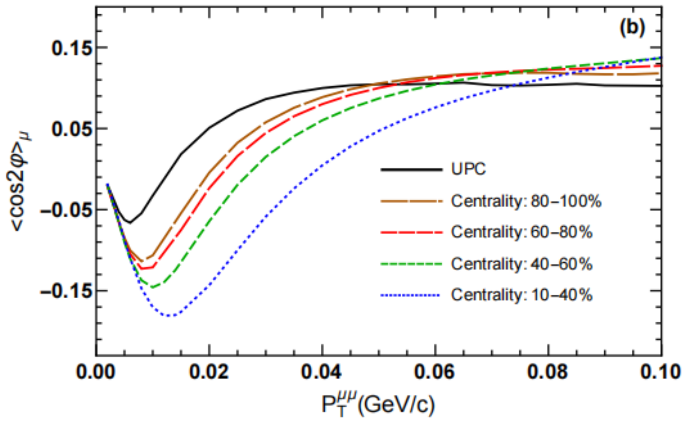

- The $\cos 2\varphi$ modulations of $\mu^+\mu^-$ are higher than e^+e^- case.

C. Li, J. Zhou, and Y.-J. Zhou, 1903.10084, 1911.00237.

Peripheral isobar collisions

$$\sigma = \frac{Z^4 e^4}{2\gamma^4 v^3} \int d^2\mathbf{b}_T d^2\mathbf{b}_{1T} d^2\mathbf{b}_{2T} \int \frac{d\omega_1 d^2\mathbf{p}_{1T}}{(2\pi)^3} \frac{d\omega_2 d^2\mathbf{p}_{2T}}{(2\pi)^3}$$
$$\times \int \frac{d^2\mathbf{p}'_{1T}}{(2\pi)^2} e^{-i\mathbf{b}_{1T}\cdot(\mathbf{p}'_{1T}-\mathbf{p}_{1T})} \frac{F^*(-\bar{p}_1'^2)}{-\bar{p}_1'^2} \frac{F(-\bar{p}_1^2)}{-\bar{p}_1^2}$$
$$\times \int \frac{d^2\mathbf{p}'_{2T}}{(2\pi)^2} e^{-i\mathbf{b}_{2T}\cdot(\mathbf{p}'_{2T}-\mathbf{p}_{2T})} \frac{F^*(-\bar{p}_2'^2)}{-\bar{p}_2'^2} \frac{F(-\bar{p}_2^2)}{-\bar{p}_2^2}$$
$$\times \int \frac{d^3k_1}{(2\pi)^3 2E_{k1}} \frac{d^3k_2}{(2\pi)^3 2E_{k2}} (2\pi)^4 \delta^{(4)}\left(\bar{p}_1 + \bar{p}_2 - k_1 - k_2\right) \delta^{(2)}\left(\mathbf{b}_T - \mathbf{b}_{1T} + \mathbf{b}_{2T}\right)$$
$$\times \sum_{\text{spin of } l,\bar{l}} \left[u_{1\mu} u_{2\nu} L^{\mu\nu}(\bar{p}_1, \bar{p}_2; k_1, k_2)\right] \left[u_{1\sigma} u_{2\rho} L^{\sigma\rho *}(\bar{p}'_1, \bar{p}'_2; k_1, k_2)\right],$$

Charge density distribution $\Rightarrow F$

Mass density distribution $\Rightarrow \int_{b_{min}}^{b_{max}} db_T$

The lepton pair photoproduction is calculated with the charge density distribution, while the centrality is defined from the Glauber model with the nuclear mass density.

Nuclear structure calculation by DFT

➢ Nuclear charge density ≠ Nuclear mass density

(a)	R_c	d_c	R_n	d_n
Ru	5.083 fm	0.477 fm	5.093 fm	0.488 fm
Zr	4.977 fm	0.492 fm	5.022 fm	0.538 fm

$$\rho_i(\mathbf{r}) \equiv \frac{C_i}{1+\exp[(|\mathbf{r}|-R_i)/d_i]}$$

c: nuclear charge density
n:nuclear mass density

S. Lin,R.J. Wang, J.F. Wang, H.J. Xu, S. Pu and Q. Wang, Phys.Rev.D 107 (2023), 054004.

Parameter setting

(a)	R_c	d_c	R_n	d_n
Ru	5.083 fm	0.477 fm	5.093 fm	0.488 fm
Zr	4.977 fm	0.492 fm	5.022 fm	0.538 fm

(b)	R_c	d_c	R_n	d_n
Ru	5.083 fm	0.477 fm	R_c^{Ru}	d_c^{Ru}
Zr	4.977 fm	0.492 fm	R_c^{Zr}	d_c^{Zr}

For comparison, we also use the charge density distribution as the mass density distribution to define the centrality

S. Lin,R.J. Wang, J.F. Wang, H.J. Xu, S. Pu and Q. Wang, Phys.Rev.D 107 (2023), 054004.

Numerical results

- P_T^{ee} distribution

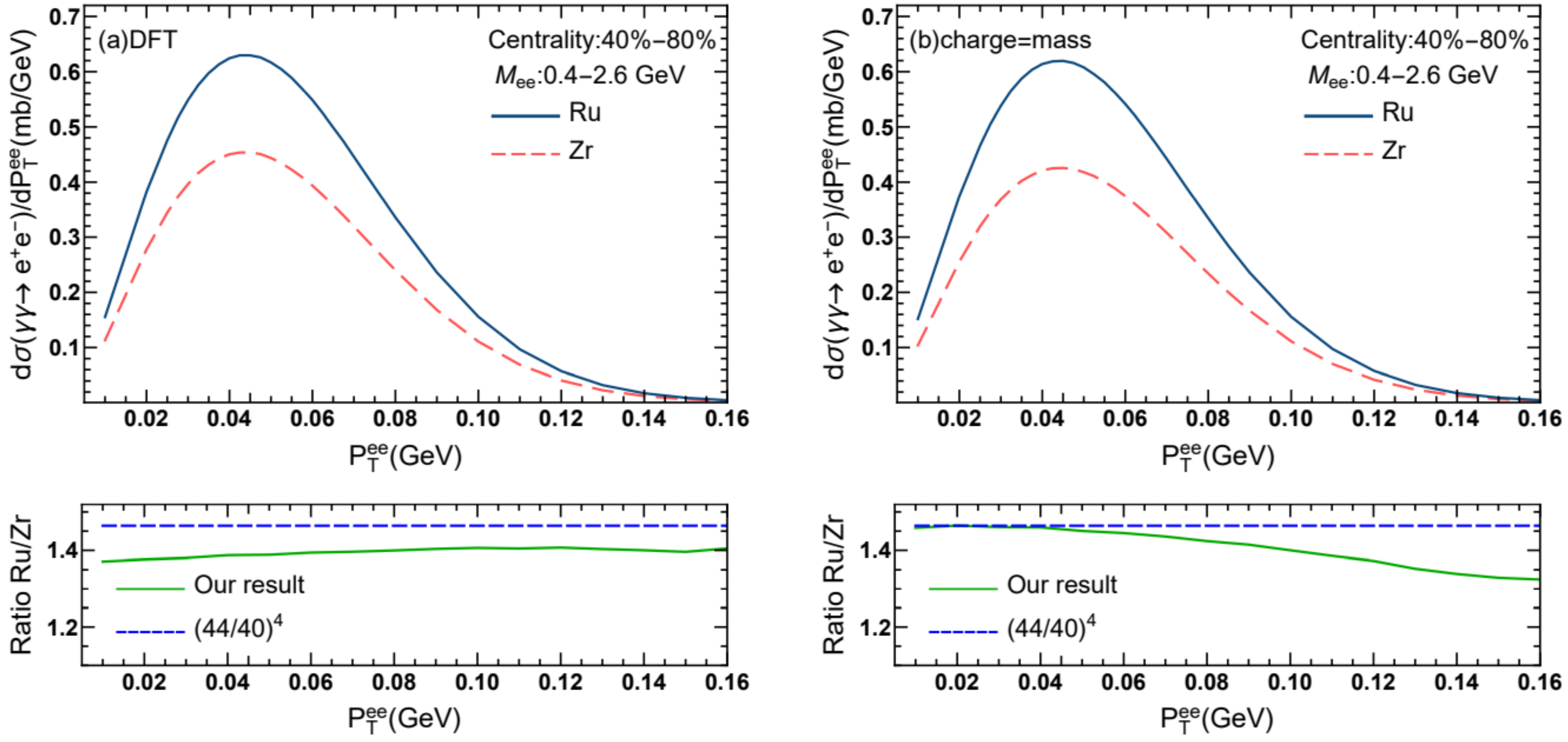

S. Lin, R.J. Wang, J.F. Wang, H.J. Xu, S. Pu and Q. Wang, Phys.Rev.D 107 (2023), 054004.

Numerical results

- Azimuthal asymmetry

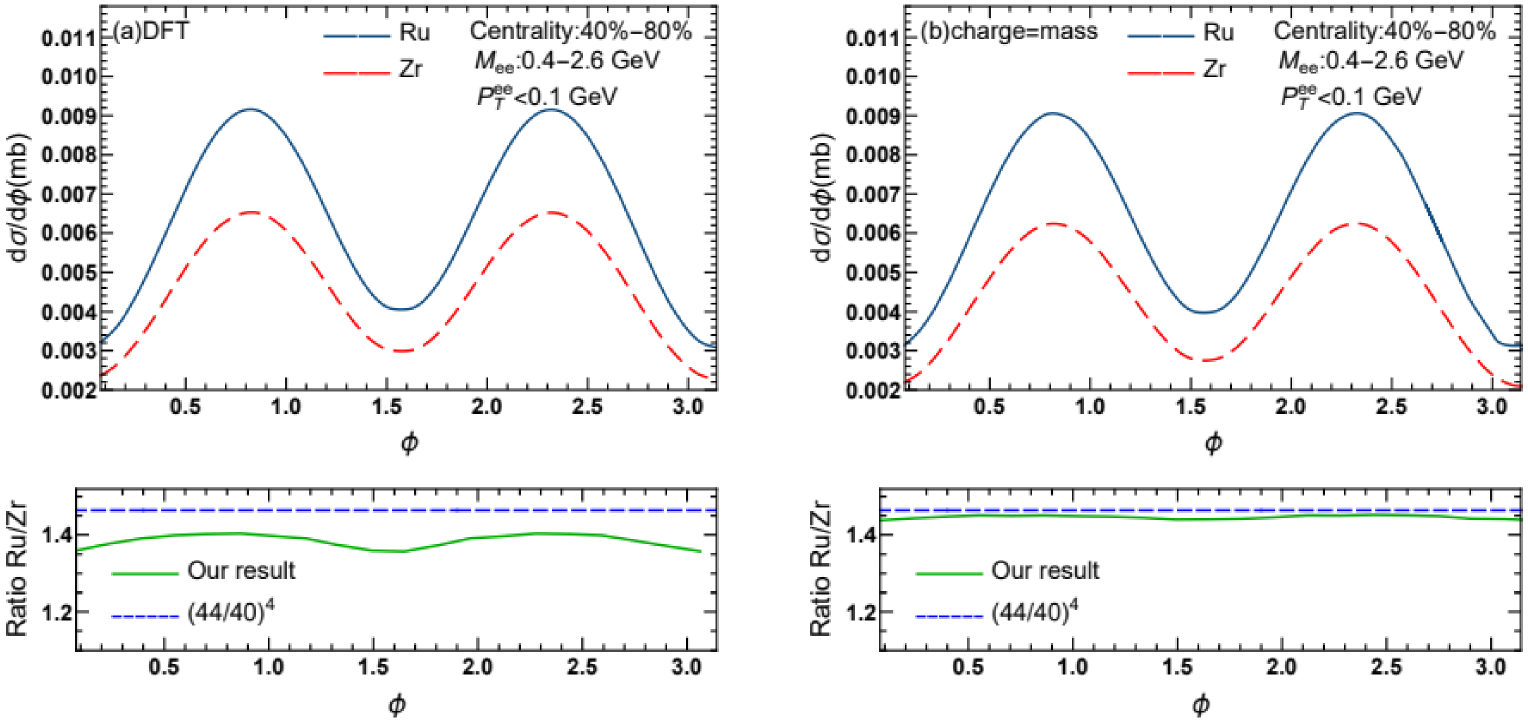

S. Lin,R.J. Wang, J.F. Wang, H.J. Xu, S. Pu and Q. Wang, Phys.Rev.D 107 (2023), 054004.

Numerical results

➢ Charge and centrality dependence

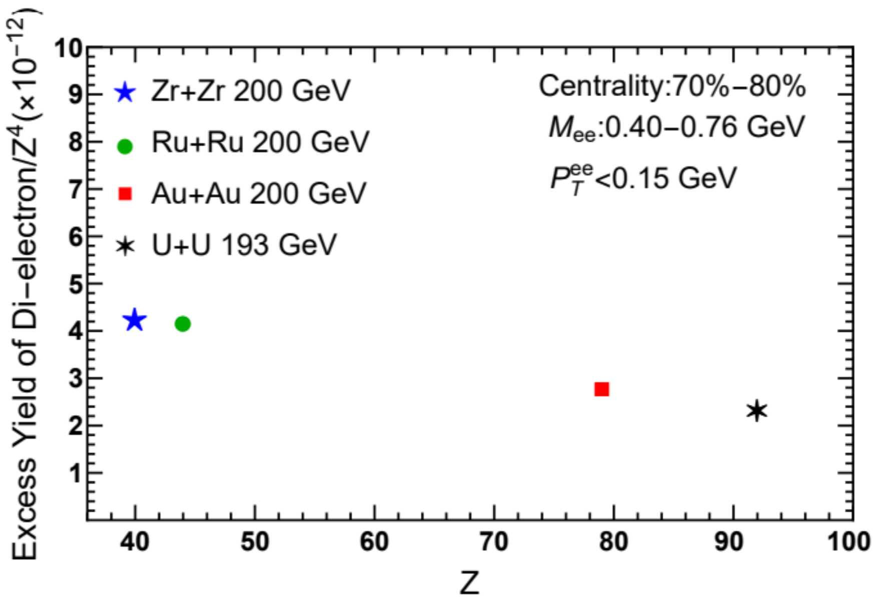

	Ru	Zr	ratio Ru/Zr
40-60%	2.328×10^{-5}	1.615×10^{-5}	1.441
60-70%	2.245×10^{-5}	1.549×10^{-5}	1.449
70-80%	2.178×10^{-5}	1.495×10^{-5}	1.457

S. Lin,R.J. Wang, J.F. Wang, H.J. Xu, S. Pu and Q. Wang, Phys.Rev.D 107 (2023), 054004.

Photoproduction of ρ in ultraperipheral isobar collisions

Photoproduction of vector meson

γ+p/A→V+p/A
- parton structure
- Gluon saturation and small x physics

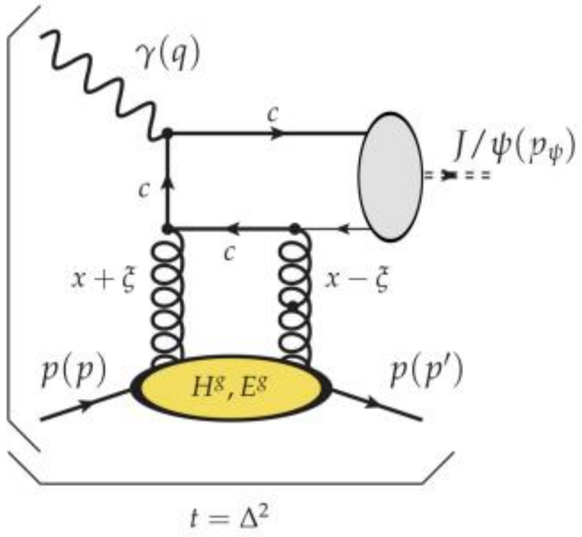

J. C. Collins, L. Frankfurt, M. Strikman, Phys. Rev. D 56, 2982 (1997).
J. Koempel, P. Kroll, A. Metz, and J. Zhou, Phys. Rev.D 85, 051502 (2012)
Y. Guo, X. Ji, and F. Yuan, (2023), 2308.13006.
S. J. Brodsky, L. Frankfurt, J. F. Gunion, A. H. Mueller,and M. Strikman, Phys. Rev. D 50, 3134 (1994).
……

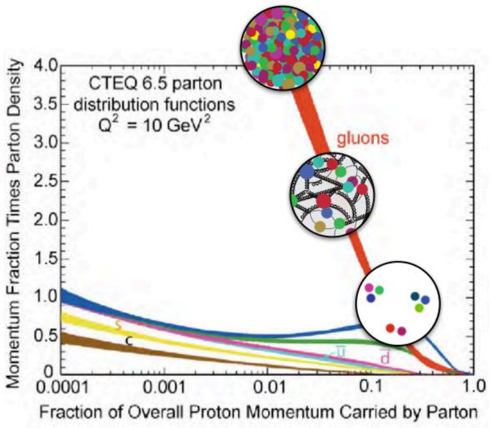

Photoproduction of vector meson

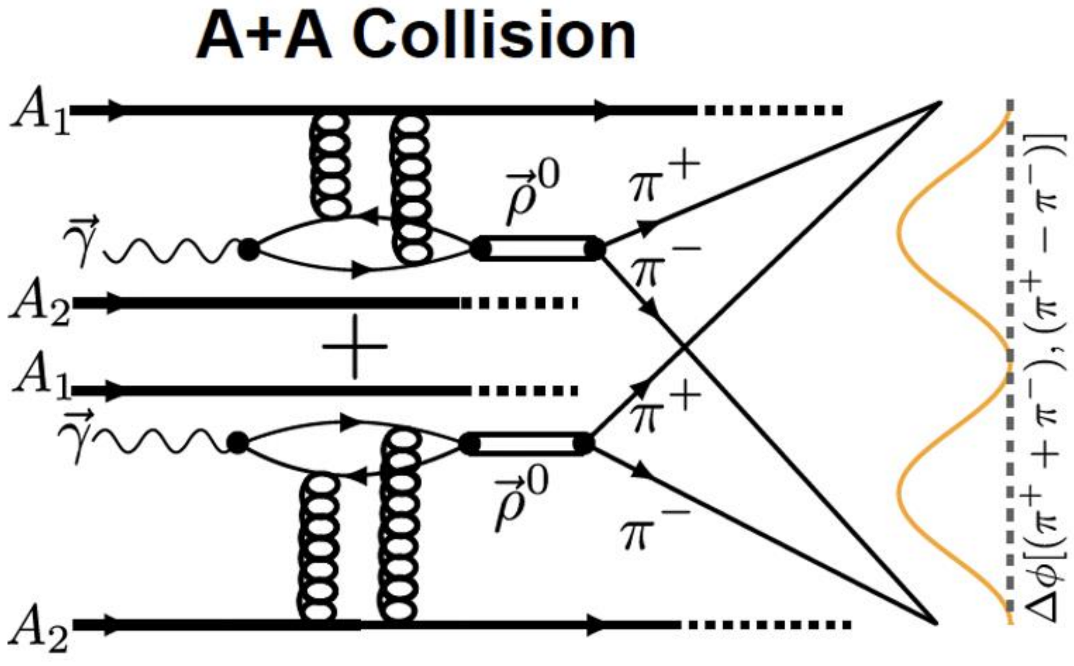

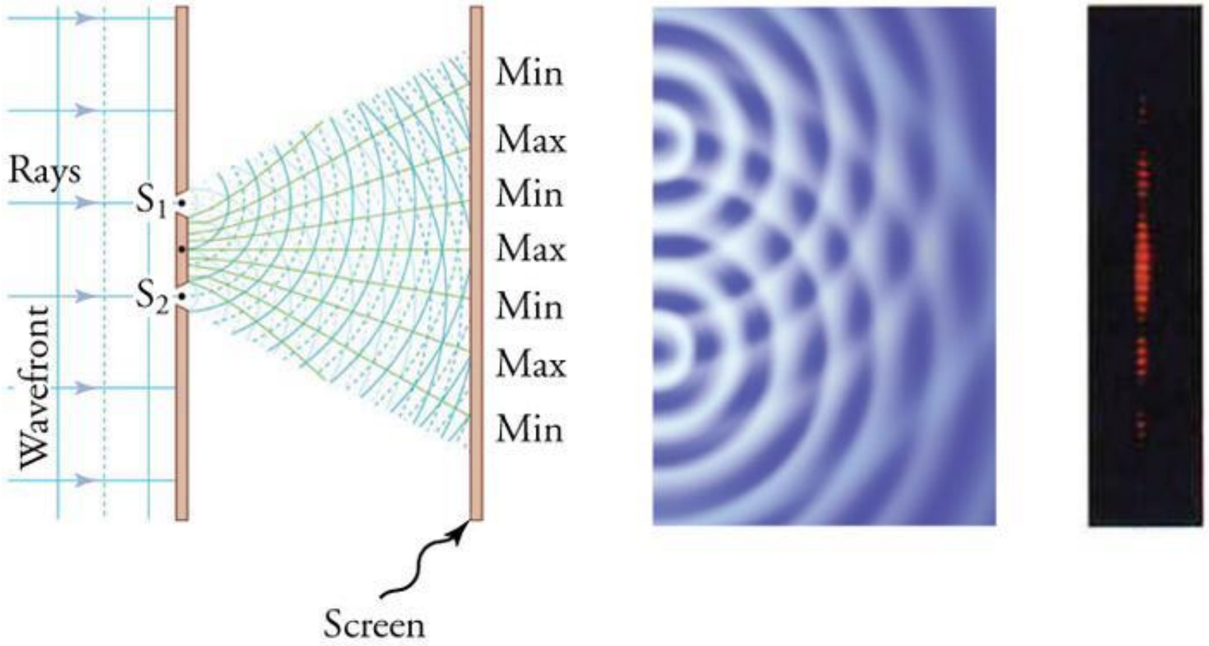

Interference effect

Photoproduction of vector meson

- $\rho^0 \to \pi^+\pi^-$
- Azimuthal asymmetries **$\cos(2\phi)$** in diffractive vector meson production in UPC

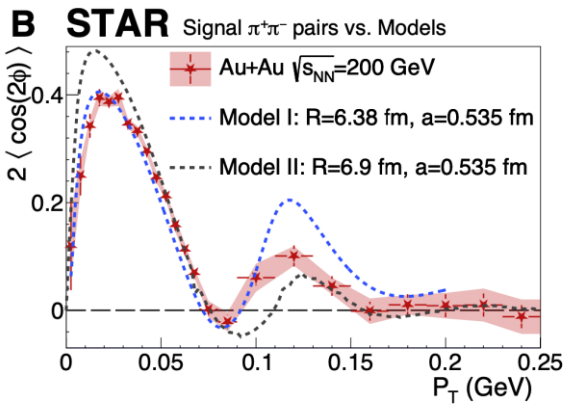

STAR: **Sci. Adv. 9, abq3903 (2023)**

Theory:

- Model I: **Zha, Brandenburg, Ruan, Tang, Xu, PRD 2021**
- Model II: **Xing, Zhang, Zhou, Zhou, JHEP 2020**

Photoproduction of vector meson

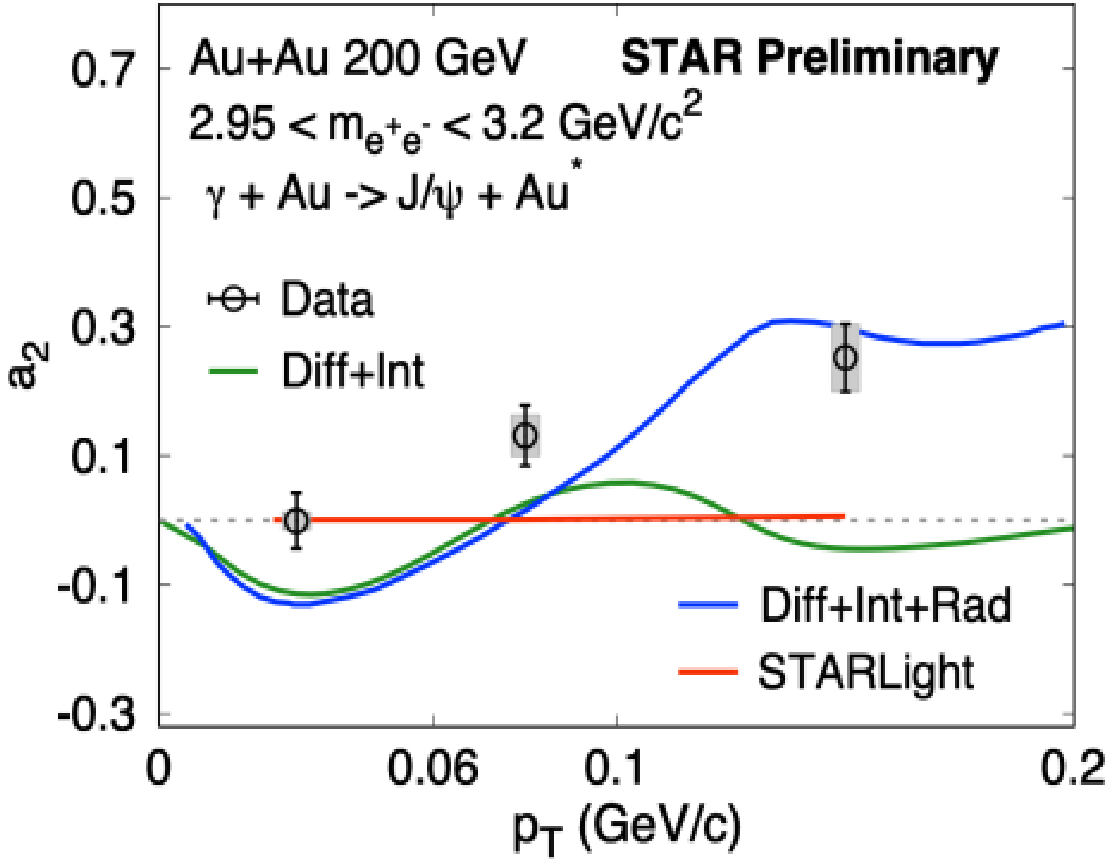

J. D. Brandenburg, Z. Xu, W. Zha, C. Zhang, J. Zhou and Y.Zhou.Phys.Rev.D 106 (2022) 7, 074008

Sudakov

Ultraperipheral isobar collisions

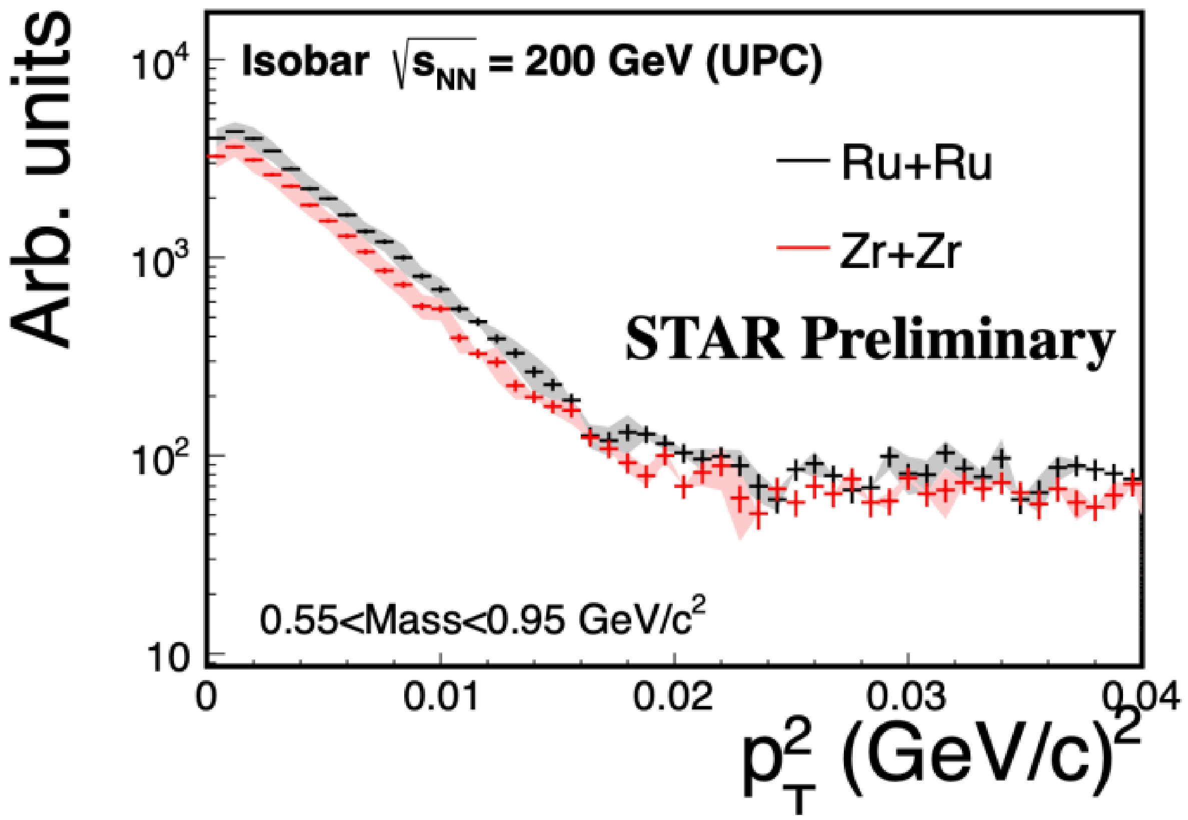

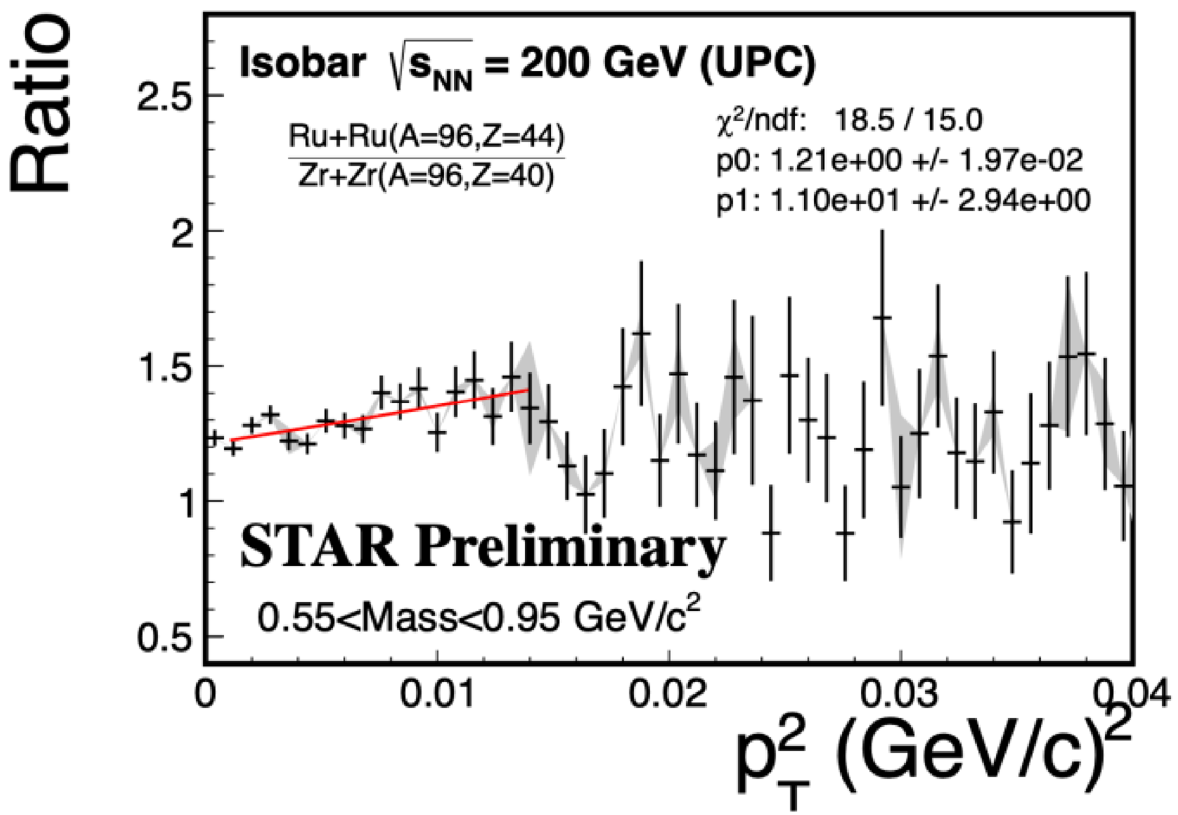

Photoproduction of vector meson

- Dipole model

$$\mathcal{A} = 2i \int d^2\mathbf{b}_T e^{i\mathbf{\Delta}_T\cdot\mathbf{b}_T} \int \frac{d^2\mathbf{r}_T}{4\pi} \int_0^1 dz \times \Psi^{\gamma\to q\bar{q}}(\mathbf{r}_T, z) N(\mathbf{r}_T, \mathbf{b}_T) \Psi^{V\to q\bar{q}*}(\mathbf{r}_T, z)$$

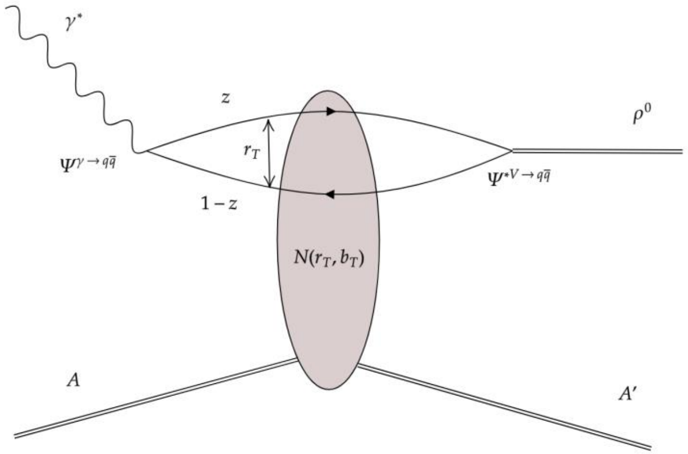

- Dipole nucleus scattering amplitude parameterization

$$N(b_\perp, r_\perp) = 1 - \frac{1}{N_c}\left\langle \mathrm{Tr}\left(U(b_\perp + r_\perp/2)U^\dagger(b_\perp - r_\perp/2)\right)\right\rangle$$

$$N(\mathbf{r}_T, \mathbf{b}_T) = 1 - \exp\left[-2\pi B_p A T_A(\mathbf{b}_T) \mathcal{N}(\mathbf{r}_T)\right]$$

$$T_A(\mathbf{b}_T) = \int dz \rho(z, \mathbf{b}_T)$$

thickness function

Nuclear deformation

- Ru deformed as an ellipsoid

  Zr deformed as a pear

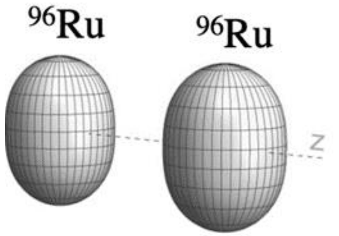

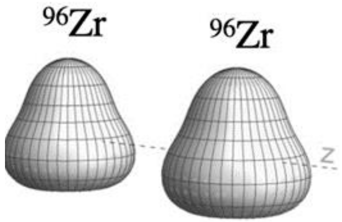

- The Woods-Saxon distribution

$$\rho(r,\theta,\phi) = \frac{\rho_0}{1+\exp\{[r-R_0(\theta,\phi)]/a\}}$$

$$R_0(\theta) = R\,[1+\beta_2 Y_{2,0}(\theta)+\beta_3 Y_{3,0}(\theta)+...]$$

β_2:quadrupole deformation
β_3:octupole deformation

Nuclear deformation

- ➢Ru deformed as an ellipsoid

  Zr deformed as a pear

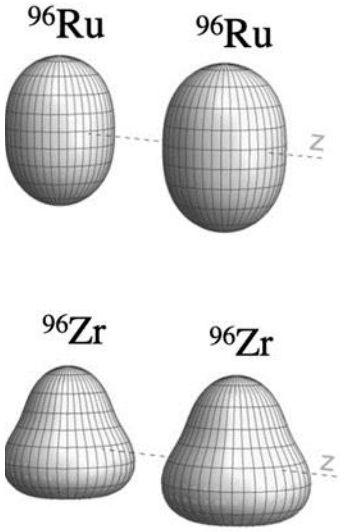

(a) with deformation	R	a	β_2	β_3
Ru	5.093 fm	0.471 fm	0.16	0
Zr	5.021 fm	0.517 fm	0	0.20

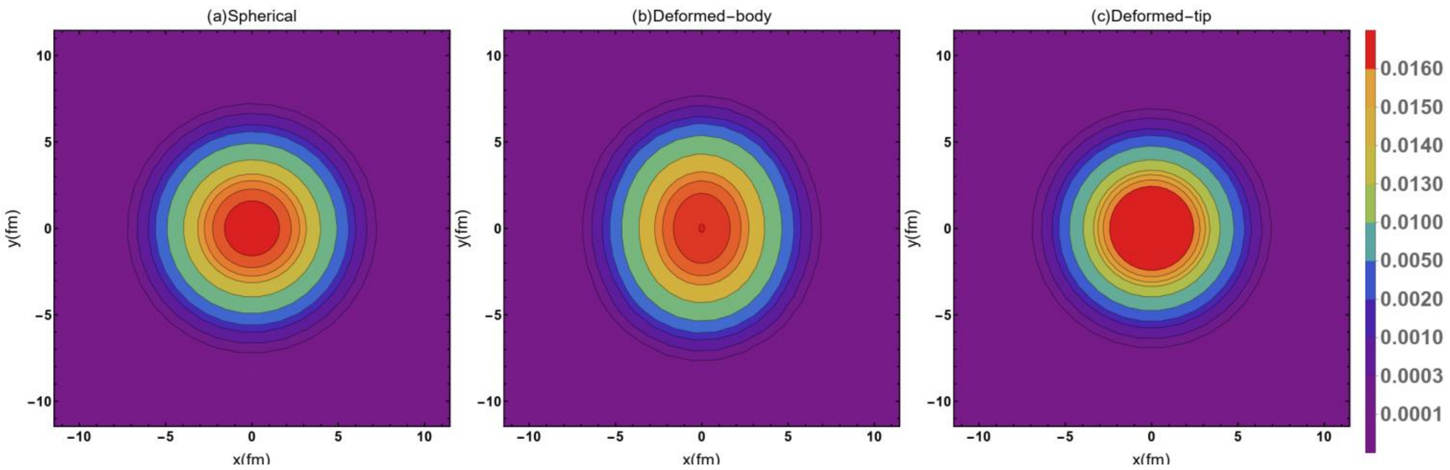

β_2:quadrupole deformation
β_3:octupole deformation

The thickness function 2D plot

Compared to the experiment

- We calculate the ratio of transverse momentum spectra of ρ^0 in isobar UPCs.(tip-tip collision, body-body collisions , deformation average, no deformation, respectively)

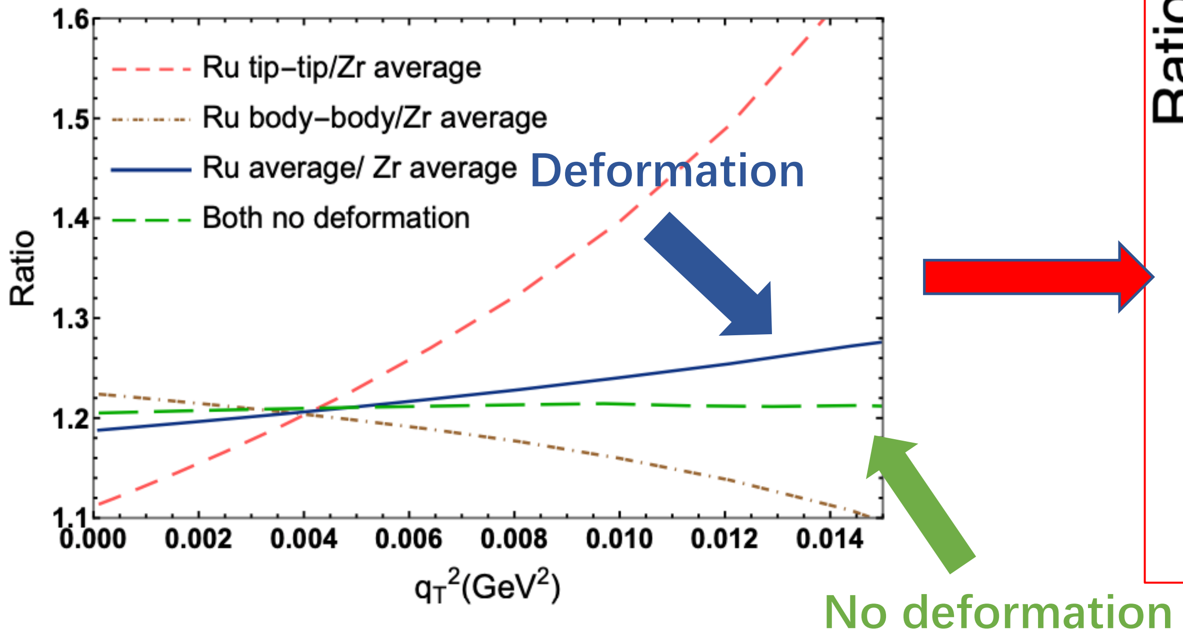

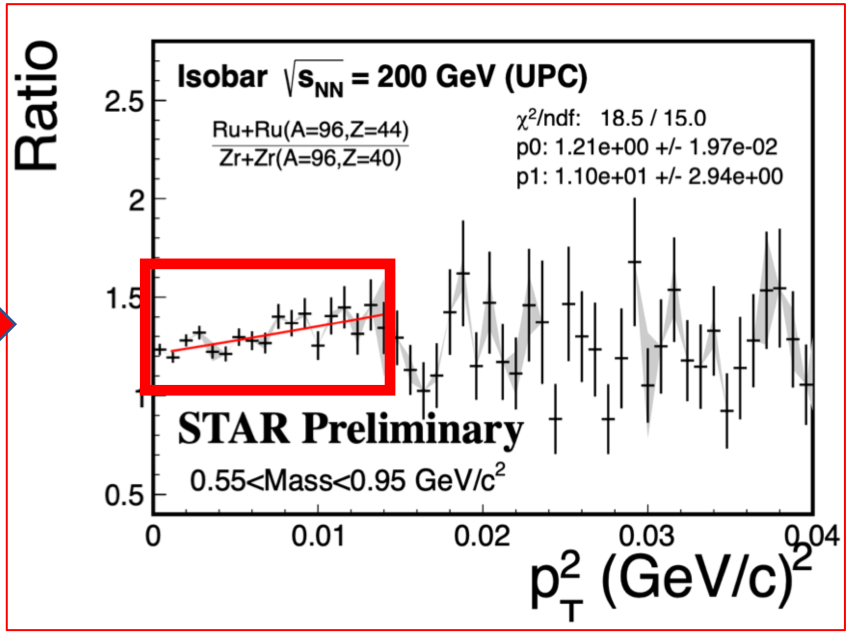

Phenomenological Explanation

- Dipole-nucleus scattering amplitude approximation

$$N(\mathbf{r}_T, \mathbf{b}_T) = 1 - \exp\left[-2\pi B_p A T_A(\mathbf{b}_T)\mathcal{N}(\mathbf{r}_T)\right] \Longrightarrow N(\mathbf{r}_T, \mathbf{b}_T) \simeq 2\pi B_p A T_A(\mathbf{b}_T)\mathcal{N}(\mathbf{r}_T)$$

- Thickness function approximated as Gaussian distribution

$T_A(\mathbf{b}_T) \sim \exp\left(-\frac{\mathbf{b}_T^2}{w_T^2}\right)$ with ω_T being the nucleus width.

- The dipole amplitude will be proportional to $e^{-\frac{1}{4}q_T^2 w_T^2}$ after the integration of b_T

$$\mathcal{A} \sim A\int \frac{d^2\mathbf{r}_T}{4\pi}\int_0^1 dz B_p \mathcal{N}(\mathbf{r}_T) \times \Psi^{\gamma\to q\bar{q}}(\mathbf{r}_T, z)\Psi^{V\to q\bar{q}*}(\mathbf{r}_T, z) \times \int d^2\mathbf{b}_T e^{i\mathbf{q}_T\cdot\mathbf{b}_T}\exp\left(-\frac{\mathbf{b}_T^2}{w_T^2}\right) \Longrightarrow \mathcal{A}(q_T^2) \propto e^{-\frac{1}{4}q_T^2 w_T^2}$$

Phenomenological Explanation

- The ratio of the transverse momentum spectra is proportional to $e^{\delta\omega_T q_T^2}$ with $\delta\omega_T = -\frac{1}{2}\times[(\omega_T^{Ru})^2 - (\omega_T^{Zr})^2]$

- No deformation → slope ≈ 0

  $\omega_T^{Ru}(tip) < \omega_T^{Zr}$ → slope > 0

  $\omega_T^{Ru}(body) > \omega_T^{Zr}$ → slope <0

	Ru (body)	Ru (tip)	Ru (spherical)	Zr (spherical)
w_T	3.628 fm	3.372 fm	3.544 fm	3.571 fm

Compared to the experiment

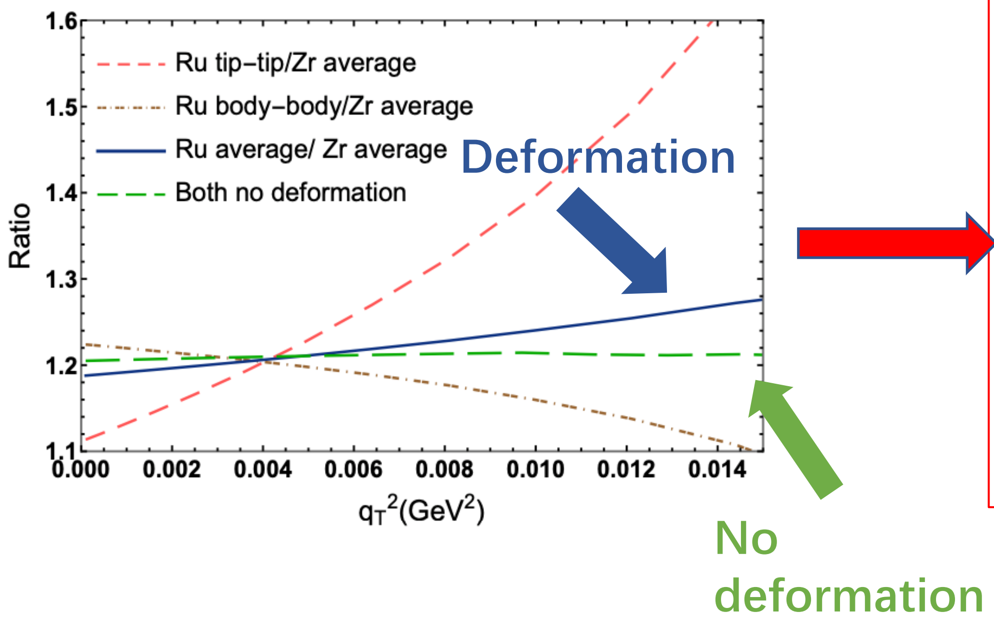

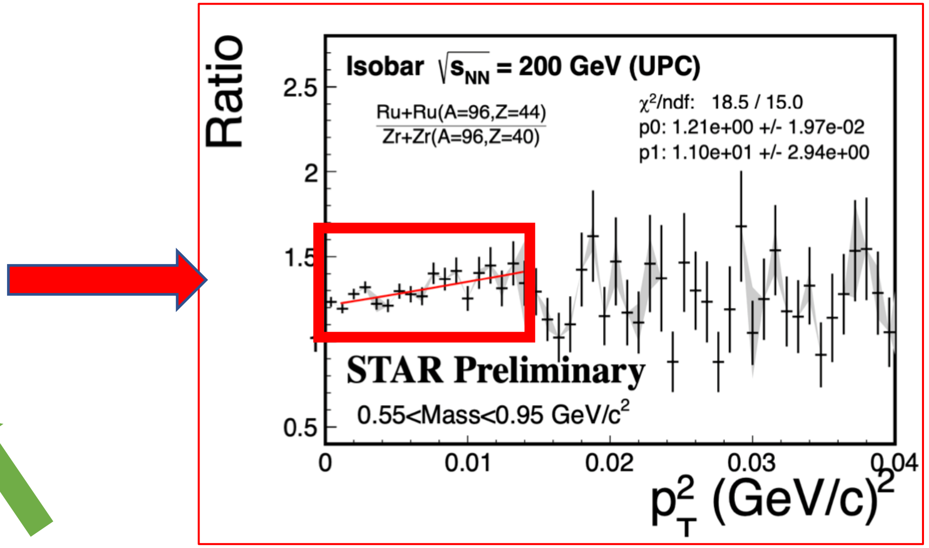

(a) with deformation	R	a	β_2	β_3
Ru	5.093 fm	0.471 fm	0.16	0
Zr	5.021 fm	0.517 fm	0	0.20

(b) without deformation	R	a	β_2	β_3
Ru	5.093 fm	0.487 fm	0	0
Zr	5.022 fm	0.538 fm	0	0

The slope of the transverse momentum spectrum ratio is sensitive to nuclear deformation

Summary

- Photoproduction of di-electrons in peripheral isobar collision

Nuclear charge density ≠ Nuclear mass density

- Photoproduction of ρ in ultraperipheral isobar collisions

Nuclear deformation

- The photoproduction in isobar collisions may provide a new way to probe the nuclear structure

Thanks for your attention!